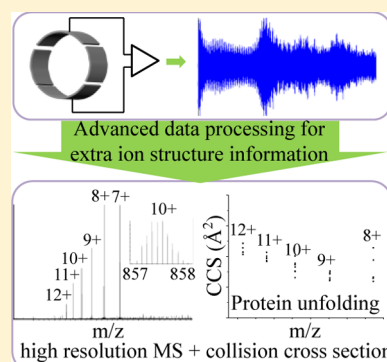


Collision Cross Section Measurements for Biomolecules within a High-Resolution Fourier Transform Ion Cyclotron Resonance Cell

Lu Mao,^{†,||} Yu Chen,^{#,||} Yi Xin,[†] Yu Chen,[‡] Li Zheng,[†] Nathan K. Kaiser,[‡] Alan G. Marshall,^{*,‡,§} and Wei Xu^{*,†}[†]School of Life Science, Beijing Institute of Technology, Beijing 100081, China[#]Shaanxi Cancer Hospital, Xian, Shaanxi 710061, China[‡]Ion Cyclotron Resonance Program, National High Magnetic Field Laboratory, Tallahassee, Florida 32310, United States[§]Department of Chemistry & Biochemistry, Florida State University, Tallahassee, Florida 32306, United States

S Supporting Information

ABSTRACT: To understand the role and function of a biomolecule in a biosystem, it is important to know both its composition and structure. Here, a mass spectrometric based approach has been proposed and applied to demonstrate that collision cross sections and high-resolution mass spectra of biomolecule ions may be obtained simultaneously by Fourier transform ion cyclotron resonance mass spectrometry. With this method, the unfolding phenomena for ubiquitin ions that possess different number of charges have been investigated, and results agree well with ion mobility measurements. In the present approach, we extend ion collision cross-section measurements to lower pressures than in prior ion cyclotron resonance (ICR)-based experiments, thereby maintaining the potentially high resolution of Fourier transform ion cyclotron resonance mass spectrometry (FTICR MS), and enabling collision cross section (CCS) measurements for high-mass biomolecules.



The conformation of a protein determines its biological activity, and even a slight change in its structure can affect its function. Therefore, the ability to resolve the primary sequence and higher-order structure¹ of a protein is critically important in proteomics, disease diagnosis, drug design, etc.² With the capability of providing both the mass-to-charge (m/z) ratio and structural information for a gas-phase ion, mass spectrometry (MS) has been widely used in protein analysis.³ A mass spectrometer measures the m/z of an ion, and its primary and higher-order structure can be probed with tandem MS techniques,⁴ in which ion activation is used to fragment precursor ions. Various MS techniques that reflect gas-phase protein conformations, include surface-induced dissociation,⁵ electron capture dissociation,⁶ and electron transfer dissociation.⁷ Methods such as ion mobility spectrometry (IMS)^{8–10} and H/D exchange¹¹ have also been employed to measure the collision cross section (CCS) and tertiary structure of a protein, and abundant results have been produced by coupling with MS instruments.^{12,5} More recently, a method for ion CCS measurements in quadrupole ion traps was also proposed theoretically based on a time-frequency analysis method.¹³ However, because of the complex and dynamic nature of protein structure, there have been increasing demands for versatile and/or complementary ion structure analysis techniques to achieve more accurate analyses.

There is considerable evidence that protein conformation, which is determined in large part by hydrogen bonds and van der Waals contacts, could be conserved in the absence of

solvent.¹⁴ It has been realized since the 1960s that the ion cyclotron resonance (ICR) mass spectral peak width can provide an experimental measure of ion-neutral CCS.¹⁵ Yang et al. recently determined ion-neutral CCSs for (e.g.) gas-phase crown ether and other complexes by measurement of 4.7 T Fourier transform ion cyclotron resonance (FTICR) MS peak width.^{16,17} Here, we extend FTICR MS measurement of CCSs to gas-phase protein ions of various charge states, which was enabled by accelerating ions to higher kinetic energies during measurements and the development of an energetic ion-neutral collision model as well as an efficient time-domain data processing method. Use of higher magnetic field strength (9.4 T vs 4.7 T) allows maintenance of high mass resolution (low buffer gas pressure) during simultaneous CCS and MS measurements with minimal or no modification of FTICR instrumentation.

Prior FTICR determinations of CCS were based on measurement of frequency-domain peak width.^{17,16} Here, we introduce an efficient time-domain data processing method to extract the ion m/z ratio and CCS simultaneously from the image current signal detected in an FTICR cell. Figure 1a provides a schematic flowchart for data acquisition and data processing. Experiments were carried out with a custom-built 9.4 T FTICR instrument with an electrically compensated ICR

Received: January 8, 2015

Accepted: March 28, 2015

Published: March 28, 2015

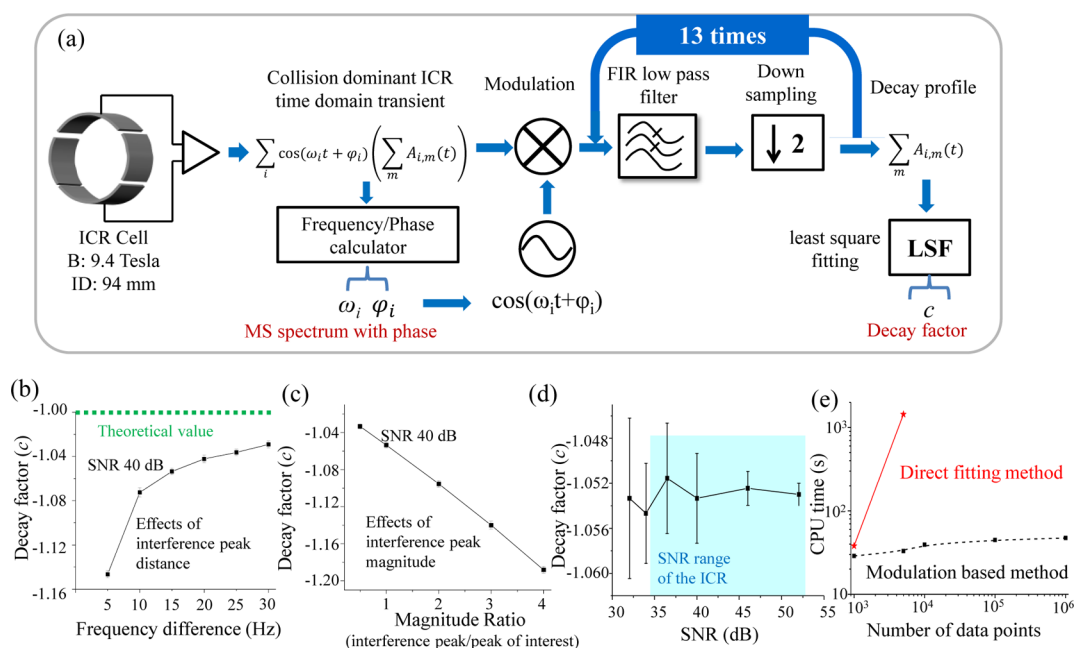


Figure 1. (a) Schematic flowchart for the experiment. Chemical noise (interference peak) effects on decay factor estimation. (b) Effect of interference peak distance from the peak of interest (equal magnitude). (c) Effect of interference peak magnitude with respect to that of the peak of interest (interference peak distance 15 Hz). (d) Electrical noise effect (interference peak distance 15 Hz, magnitude 1). (e) Data processing times for the current method and the conventional direct fitting method.

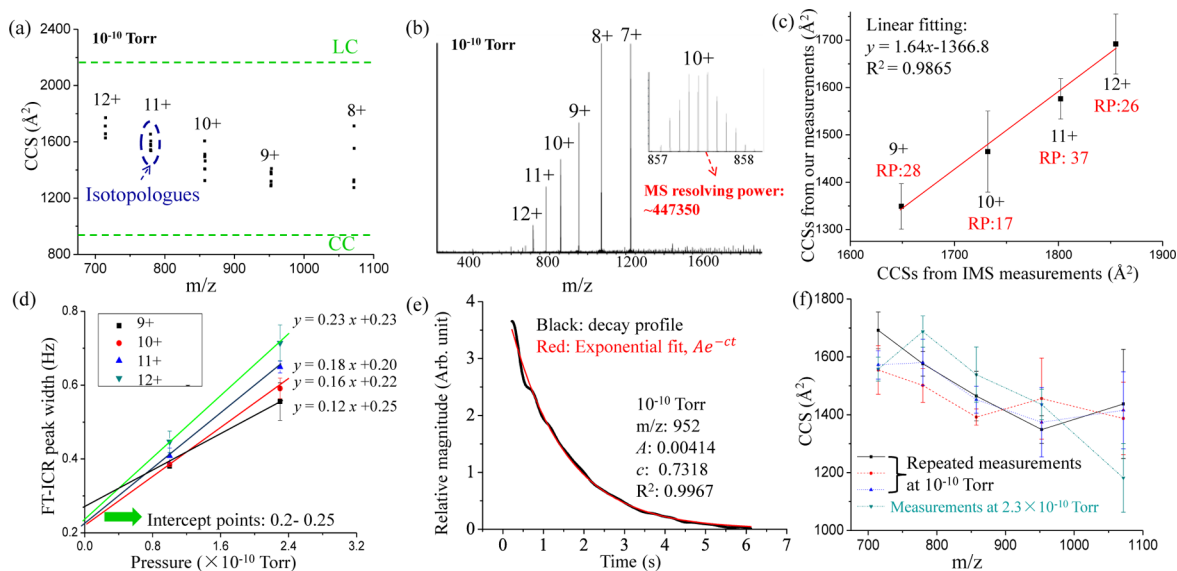


Figure 2. (a) CCSs of ubiquitin ions (see text for detail). The dashed lines are the calculated CCSs for the near linear conformer (LC) and crystal conformer (CC). (b) The corresponding mass spectrum of ubiquitin. (c) Linear correlation between the CCSs obtained in this study and the CCSs from IMS measurements. RP: resolving power of the CCS measurements, calculated as mean/std. (d) Correlation between ICR peak width and pressure. (e) Extracted decay profile versus exponential fit. (f) Repeated measurements of CCSs for ubiquitin ions.

cell.^{18–20} A pulsed leak valve controlled N_2 buffer gas pressure in the ICR cell. Data processing operated like a radio receiver. First, a fast Fourier transform (FFT)^{21,22} was performed on the image current signal to acquire a frequency-domain spectrum (ω), from which the ion m/z ratio could be determined. After selecting an ion of interest, the initial phase of the corresponding mass (peak) was calculated (Figure S1 in the Supporting Information). From frequency and phase values, the image current signal was then modulated, so that the frequency of interest was shifted to zero (Figure S2 in the Supporting Information). A multistep low pass filtering and down-sampling

process (13 rounds) was then carried out to carefully remove other mass peaks and noises from the transient signal. In this process, minimum distortion of the peak of interest is very important. Next, the decay profile ($A_{i,m}(t)$) was fed into a least-squares fitting module to calculate the decay rate (see the Supporting Information). (A similar method about least-squares fitting has recently been published independently by Aushev et al.)²³ Finally, the CCS of the ion of interest could be calculated from the time-domain signal decay rate constant (eq 1, see below).

Accuracy and performance of the data processing method were characterized from simulated data (see the Supporting Information for details). Two major factors affect accuracy: electrical noise and chemical noise. As shown in Figure S3 in the Supporting Information, flicker noise and Gaussian white noise are the major components of the electrical noise. Chemical noise is a result of interference between isotope peaks and mass peaks from other chemicals. As plotted in Figure 1b–d, electrical noise is the major source of the variation of estimated decay factor ($\sim 1\%$ variation in CCS for a signal-to-noise ratio of 40 dB); whereas chemical noise causes deviations of estimated decay factor ($\sim 5\%$ deviation if the interference peak has the same magnitude as that of the peak of interest and 15 Hz away). Compared to conventional direct fitting methods (details in the Supporting Information), data processing speed of the current method (less than 1 min) is significantly faster (see Figure 1e) and is capable of handling more than 8 million time-domain data points as shown in later sections.

With this method, the unfolding of ubiquitin ions was investigated with the results shown in Figure 2. As indicated in Figure 1a, the image current decay needs to be dominated by ion-neutral collisions; thereby, effects from other factors need to be minimized such as space charge, electric and magnetic field imperfections, etc. To achieve that purpose, cell pressure, total ion number, signal transient length, number of data point, cell diameter, and ion excitation radius were carefully controlled: pressure in the ultrahigh vacuum region of the instrument was maintained between 10^{-10} and 5.9×10^{-9} Torr; total number of ions in the cell was controlled by external accumulation (40 ms) in an octopole ion trap; transient signal length was set at 6.115 s (8388608 data points); inner diameter (ID) of the ICR cell is 94 mm; ions were excited to 40% of the cell radius for image current detection. With the current instrument setup, a ubiquitin ion (10+ charge state, $m/z \sim 857$) has a kinetic energy of ~ 17.5 keV after excitation, and the maximum exchange energy available during a single ion-neutral collision is ~ 114 eV (see the Supporting Information for details). Therefore, a single collision should dephase a ubiquitin ion from the spatially coherent ion packet. Thus, an energetic hard-sphere ion-neutral collision model was used to calculate CCSs from the decay factors (details in Guo et al.²⁴),

$$c = nv\sigma = \frac{P}{kT} \frac{9.648 \times 10^7 Br}{m/z} \sigma, \quad A(t) = A_0 e^{-ct} \quad (1)$$

in which c denotes time-domain ICR signal exponential decay time constant, n is buffer gas density, v is ion velocity, σ is ion-neutral CCS, P is pressure, k is Boltzmann constant, T is temperature, B is magnetic field, r is ion cyclotron orbital radius, $A(t)$ is time-domain ICR signal profile, and A_0 is ICR signal amplitude.

Each data point in Figure 2a represents the calculated CCS for an isotopic peak of certain charge state in the mass spectrum. It is known that a protein ion will typically unfold further (i.e., exhibit larger CCS) with increasing charge state due to Coulomb repulsion, as confirmed by our measurements for ubiquitin (see Figure 2a). As shown in Figure 2b, another advantage of the current method is the simultaneous generation of a high-resolution mass spectrum due to the low cell pressure, with a mass resolving power, $m/\Delta m_{50\%} = \sim 450\,000$ for ions of m/z 857.576. (in which $\Delta m_{50\%}$ is FTICR MS peak full width at half-maximum peak height) The presence of heavy atoms (^{13}C , ^{15}N) should not affect the CCS determination. Thus, CCS

mean and standard deviation (std) can be calculated for ubiquitin ions of a given charge state (Figure 2c,f). As noted, the CCS values determined in the present study are systematically shifted by $\sim 300 \text{ \AA}^2$ smaller relative to those measured by IMS.²⁵ Furthermore, slope of the correlation line in Figure 2c is not 1.00 but 1.64. The CCS deviation may be attributed to the estimated error of the data processing method and pressure reading uncertainty inside the ICR cell. In addition, the ion-neutral collision energies for the IMS and FT-based methods differ significantly. IMS is normally performed at relatively low ion-neutral collision energies, whereas the FT-based method is conducted at a much higher energy level (keV). Ion CCS may be energy dependent: for instance, the ion mobility constant in an IMS experiment is highly sensitive to collision conditions (temperature and electric field strength).^{26,27} Therefore, the CCSs measured by the two methods are different, suggesting that the two methods could be complementary for ion structure analysis.

Gaussian noise is believed to account for the relatively low CCS resolving power (~ 20). As shown in Figure 2b, the SNR and amplitude for each isotopic peak are different, leading to different estimated deviation in the decay factor: e.g., in Figure 1c,d ($4\text{--}20\%$ estimated deviation as the magnitude ratio varies from 1 to 4). As a result, standard deviation in the estimated CCSs for isotopic peaks is relatively large. IMS measurements have demonstrated that both 7+ and 8+ charge states of ubiquitin exhibit two conformations, accounting for the large CCS standard deviation for the 8+ ions.²¹ The pressure dominant signal decay condition was further confirmed. Figure 2d,e and Figure S6 in the Supporting Information suggest that the signal decay is pressure dominant for ubiquitin ions for the following reasons: (1) CCS increases linearly with pressure (Figure 2d); (2) the interception points in Figure 2d are the expected ICR peak width without ion-molecule collisions, consistent with the FFT peak width (~ 0.198 Hz) of a 6.115 s long time-domain ICR signal (see the Supporting Information for details); (3) the extracted decay profile agrees well with the theoretical exponential decay model ($R^2 > 0.99$ in Figure 2e); and (4) when the pressure is further elevated (above 5×10^{-10} Torr), ubiquitin ions were not observed in the mass spectra (Figure S6 in the Supporting Information). Experiments were repeated three times as well as at different pressures as shown in Figure 2f.

Additional experimental and calculation results in the Supporting Information illustrate that the signal decay was dominated by buffer gas pressure (“high-pressure limit”) based on isolated mass spectra of ubiquitin, ion mean free path calculation, the independence of ion number, and decay factor. Measurements of cytochrome C, MRFA, and Ultramar were also performed, and detailed discussions are included in the Supporting Information. In general, under conditions of controlled number of ions and the energetic hard-sphere collision model, higher pressure is needed to ensure pressure-limited decay for ions of smaller CCSs: e.g., above 7.4×10^{-10} Torr for MRFA and Ultramar, compared to 10^{-10} Torr for ubiquitin and cytochrome C. Moreover, because large ions have more degrees of freedom to dissipate collisional energy, a single collision may not be sufficient to dephase a large ion from the ion coherent packet.

In this proof-of-principle study, CCS and high-resolution MS measurements were performed simultaneously in a modern FTICR cell for biomolecules. Although, many questions and challenges remain, such as the extent of application,

fundamental dephasing process during the energetic collision; a mixture of large and small ions cannot be measured at the same pressure condition (limited mass range); low CCS resolving power (inability to differentiate isomers), the present method could potentially provide a complementary tool for ion CCS measurements. Furthermore, note that CCSs measured at high collision energies in this study are systematically smaller than those measured at low collision energies in conventional IMS experiments. The idea also applies to any FT-based ion trap, quadrupole ion trap, and Orbitrap.^{28,29}

EXPERIMENTAL SECTION

Ubiquitin, cytochrome *c*, and Ultramark were purchased from Sigma-Aldrich (St. Louis, MO). Samples were used without further purification. Electrosprayed samples (except Ultramark) were diluted to 1 μM /L in methanol/water 1:1 v/v, 0.1% formic acid. FTICR instrument control, data acquisition, and frequency-domain data analysis are carried out with a modular ICR data station.³⁰ The time-domain ICR signal is Hanning apodized without zero-filling and Fourier transformed to produce a magnitude-mode spectrum that is converted to a *m/z* ratio by a two term calibration equation.^{31,32}

ASSOCIATED CONTENT

Supporting Information

Description of the time-domain data processing method, FTICR data noise contributions, direct fitting method, energetic hard-sphere ion-neutral collision model, high-pressure limit, ubiquitin CCSs. This material is available free of charge via the Internet at <http://pubs.acs.org>.

AUTHOR INFORMATION

Corresponding Authors

*E-mail: weixu@bit.edu.cn. Phone: +86-010-68918123.

*E-mail: marshall@magnet.fsu.edu.

Author Contributions

[†]Lu Mao and Yu Chen contributed equally to this work.

Notes

The authors declare no competing financial interest.

ACKNOWLEDGMENTS

This research was supported by NNSF China (Grants 21205005 and 21475010), MOST China (Grant 2011YQ0900502), 1000 plan, NSF (Grants DMR-11-57490 and CHM-1019193), and the State of Florida.

REFERENCES

- (1) Bowie, J. U.; Luthy, R.; Eisenberg, D. *Science* **1991**, 253, 164–170.
- (2) Aebersold, R.; Mann, M. *Nature* **2003**, 422, 198–207.
- (3) Domon, B.; Aebersold, R. *Science* **2006**, 312, 212–217.
- (4) McLafferty, F. W. *Science* **1981**, 214, 280–287.
- (5) Zhou, M.; Dagan, S.; Wysocki, V. H. *Angew. Chem., Int. Ed.* **2012**, 51, 4336–4339.
- (6) Breuker, K.; Oh, H.; Horn, D. M.; Cerda, B. A.; McLafferty, F. W. *J. Am. Chem. Soc.* **2002**, 124, 6407–6420.
- (7) Syka, J. E. P.; Coon, J. J.; Schroeder, M. J.; Shabanowitz, J.; Hunt, D. F. *Proc. Natl. Acad. Sci. U.S.A.* **2004**, 101, 9528–9533.
- (8) Hill, H. H., Jr.; Siems, W. F.; St. Louis, R. H. *Anal. Chem.* **1990**, 62, 1201A–1209A.
- (9) Ruotolo, B. T.; Hyung, S. J.; Robinson, P. M.; Giles, K.; Bateman, R. H.; Robinson, C. V. *Angew. Chem., Int. Ed.* **2007**, 46, 8001–8004.
- (10) Wyttenbach, T.; Pierson, N. A.; Clemmer, D. E.; Bowers, M. T. *Annu. Rev. Phys. Chem.* **2014**, 65, 175–196.
- (11) Breuker, K.; McLafferty, F. W. *Proc. Natl. Acad. Sci. U.S.A.* **2008**, 105, 18145–18152.
- (12) Horn, D. M.; Breuker, K.; Frank, A. J.; McLafferty, F. W. *J. Am. Chem. Soc.* **2001**, 123, 9792–9799.
- (13) He, M.; Guo, D.; Chen, Y.; Xiong, X.; Fang, X.; Xu, W. *Analyst* **2014**, 139, 6144–6153.
- (14) Oomens, J.; Polfer, N.; Moore, D. T.; van der Meer, L.; Marshall, A. G.; Eyler, J. R.; Meijer, G.; von Helden, G. *Phys. Chem. Chem. Phys.* **2005**, 7, 1345–1348.
- (15) Wobschall, D.; Graham, J. R., Jr.; Malone, D. P. *Phys. Rev.* **1963**, 131, 1565.
- (16) Yang, F.; Jones, C. A.; Dearden, D. V. *Int. J. Mass Spectrom.* **2014**, DOI: 10.1016/j.ijms.2014.07.026.
- (17) Yang, F.; Voelkel, J. E.; Dearden, D. V. *Anal. Chem.* **2012**, 84, 4851–4857.
- (18) Andersen, J. S.; Lam, Y. W.; Leung, A. K.; Ong, S.-E.; Lyon, C. E.; Lamond, A. I.; Mann, M. *Nature* **2005**, 433, 77–83.
- (19) Jones, W.; Boissel, P.; Chiavarino, B.; Crestoni, M. E.; Fornarini, S.; Lemaire, J.; Maitre, P. *Angew. Chem., Int. Ed.* **2003**, 42, 2057–2059.
- (20) Kaiser, N. K.; Savory, J. J.; McKenna, A. M.; Quinn, J. P.; Hendrickson, C. L.; Marshall, A. G. *Anal. Chem.* **2011**, 83, 6907–6910.
- (21) Cooley, J. W.; Tukey, J. W. *Math. Comput.* **1965**, 19, 297–301.
- (22) Verdun, F. R.; Giancaspro, C.; Marshall, A. G. *Appl. Spectrosc.* **1988**, 42, 715–721.
- (23) Aushev, T.; Kozhinov, A.; Tsybin, Y. J. *Am. Soc. Mass Spectrom.* **2014**, 25, 1263–1273.
- (24) Guo, D.; Xin, Y.; Xu, W. *Phys. Chem. Chem. Phys.* **2015**, 17, 9060–9067.
- (25) Valentine, S. J.; Counterman, A. E.; Clemmer, D. E. *J. Am. Soc. Mass Spectrom.* **1997**, 8, 954–961.
- (26) Hill, H. H., Jr.; Siems, W. F.; St. Louis, R. H.; McMinn, D. G. *Anal. Chem.* **1990**, 62, 1201A–1209A.
- (27) Mason, E. A.; McDaniel, E. W. In *Transport Properties of Ions in Gases*; Wiley-VCH Verlag GmbH & Co. KGaA: Weinheim, Germany, 2005.
- (28) Hu, Q.; Noll, R. J.; Li, H.; Makarov, A.; Hardman, M.; Cooks, R. G. *J. Mass Spectrom.* **2005**, 40, 430–443.
- (29) Xu, W.; Maas, J. B.; Boudreau, F. J.; Chappell, W. J.; Ouyang, Z. *Anal. Chem.* **2010**, 83, 685–689.
- (30) Blakney, G. T.; Hendrickson, C. L.; Marshall, A. G. *Int. J. Mass Spectrom.* **2011**, 306, 246–252.
- (31) Leford, E. B.; Rempel, D. L.; Gross, M. L. *Anal. Chem.* **1984**, 56, 2744–2748.
- (32) Shi, S. D. H.; Drader, J. J.; Freitas, M. A.; Hendrickson, C. L.; Marshall, A. G. *Int. J. Mass Spectrom.* **2000**, 195–196, 591–598.